Journal of Sailing Technology, Article 2016-01.

RANS BASED CFD INVESTIGATION OF THE INTERFERENCE BETWEEN TWO BOATS SAILING UPWIND

Christoph Boehm
University of Applied Sciences Kiel, Yacht Research Unit Kiel, GER

Kai Graf
University of Applied Sciences Kiel, Yacht Research Unit Kiel, GER

Manuscript received September 12, 2013; revision received June 6, 2016; accepted August 2, 2016.

Abstract: Two sailboats sailing in close proximity will influence each other's wind field. Depending on their relative positions, positive or negative aerodynamic interference may occur. This phenomenon is generally known to sailors and well understood in a qualitative manner. However, it is of great value for aerodynamicists, performance analysts and tacticians to gain a quantitative understanding of this phenomenon. Modern CFD methods allow extensive flow visualization and are therefore helpful to improve our understanding of flow interference.

This paper describes the results of numerical simulations of the aerodynamic interference of two *Elliot 6m* sailboats sailing upwind. The simulations were performed using methods based on the solution of the Reynolds Averaged Navier Stokes Equations, so called RANSE-solvers. A broad range of relative positions of the two sailboats were investigated and the differences in boat speed were quantified. The results show that, for a situation where the two boats sail directly abeam of each other, neither of them has an advantage. However, for a situation where the boats sail even with respect to a regatta start line, the leeward boat is able to achieve a quite large speed advantage of 0.2 knots.

Keywords: aerodynamics, computational fluid dynamics, sails, tactics, sail sailboat interference.

NOMENCLATURE

A_{Sails}	Sail area
c_D	Drag coefficient
c_L	Lift coefficient
C_T	Thrust or driving force coefficient
F_D	Aerodynamic drag
F_L	Aerodynamic lift
p	Pressure
p_A	Ambient pressure
v_A	Apparent wind speed
v_s	Boat speed
v_T	True wind speed
y^+	Dimensionless wall scale
z	Height above water plane
z_0	Base roughness
β_A	Apparent wind angle

β_T True wind angle

γ_S Leeway angle

φ Heel angle

INTRODUCTION

Tactical maneuvers are an important component of sailboat racing and, if properly used, allow the sailors to hold off trailing opponents or catch up with leading ones. It is therefore interesting to be able to identify, verify and quantify favorable tactical positions. With this knowledge, guidelines can be developed which can be integrated into performance analysis and shared with both coaches and sailors.

Richards (2013) investigated the aerodynamic interference of two sailboat models using wind tunnel experiments. In the experiments, one sailboat was placed on the balance while a second sailboat was placed in proximity. The position of the second sailboat was varied systematically, while the aerodynamic forces on the first sailboat were measured. As a result, Richards (2013) provided a diagram describing the aerodynamic forces generated by the first sailboat depending on the location of the second.

A similar approach was used in the study presented here; however, the method to investigate aerodynamic forces is based on RANSE-flow simulations. The focus of this study was the upwind sailing situation. As in the experiments by Richards (2013) two sailboats were investigated, with one sailboat in a fixed position and the second in proximity with varied systematically around it.

The objective of this study was to quantify the magnitude and extent of the aerodynamic interference of two sailboats sailing upwind in close proximity. The simulations not only allowed for assessing the interference between two sailboats in the most well-known leebow position, and in a range of other positions, but also it gives insight into velocity fields and pressure patterns. In addition, another benefit of the simulation was ability to compute the aerodynamic forces on both sailboats.

DESIGN OF EXPERIMENT

Entering the leebow position is a known tactical maneuver used in sailboat racing. It can be used by a leading sailboat to slow down another sailboat or force it to tack or bear away. The general idea is that, as depicted in Figure 1, a boat places itself ahead and to leeward of a windward boat. This will cause a deflection of the incident airflow for the windward as well as for the leeward boat. In particular, the apparent wind angle on the leeward boat will increase, allowing it to either point higher or generate more driving force if maintaining course. The windward boat is forced to point lower relative to the true wind or lose driving force. Any racing sailor knows that this is not a beneficial position for the windward boat, which has to tack away to get clear wind.

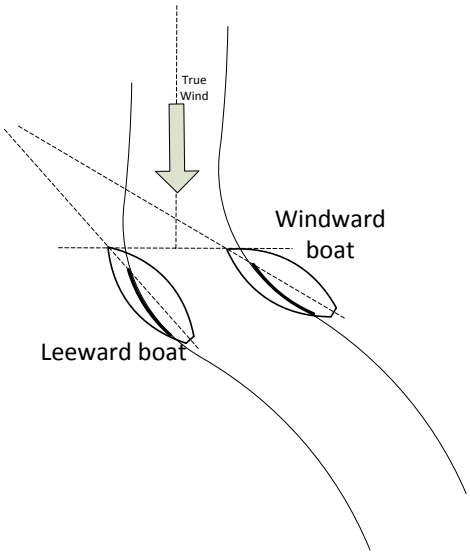

Figure 1. Sketch of leebow position.

The *Elliot 6m*, one of the sailboat classes at the Olympic Games in London 2012, was modeled in this study. The two boats were investigated at various positions relative to each other, as shown in Figure 2. One boat, the target boat (the fixed boat in Figure 2), was kept at a fixed position, while the position of the second boat (the repositioned boat in Figure 2) was varied on a rectangular grid. A rectangular grid was chosen because it allows for an easier placement of the boats as opposed to, for instance, a polar pattern. The longitudinal and transverse distance between the two boats was normalized using the boat's aerodynamic span, the distance from the water plane to the main sail headboard.

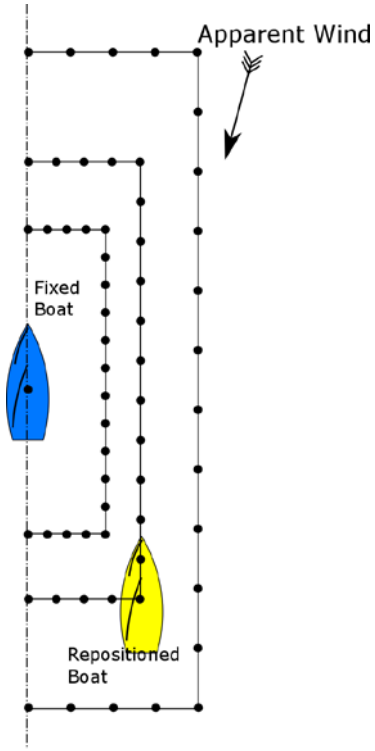

Figure 2. Matrix of boat relative positions.

The study makes use of existing symmetry conditions. The results can be diagonally mirrored, thus reducing the computational effort. The test matrix consisted of 5 half-rectangular paths with 24 positions each, resulting in 120 test points. The distance between the boats varied between 0.44 times span to 3.46 times span.

The numerical model of the flow around the two *Elliot 6m* sailboats consists of infinitely thin sails, the hull, mast, and boom. The main parameters of the *Elliot 6m* are shown in Table 1. Figure 3 shows a rendered view of the geometry. Figure 4 shows horizontal sections through the mainsail and jib, starting at the tack of the jib and ending at the mainsail headboard. The mainsail boom is sheeted at an angle of 18.5° with respect to the center line and a twist angle of 4.3°, while the jib is sheeted at an angle of 18.5° with a twist angle of 12.0°. The camber depth of both sails varies from 8 to 12% over the span, with the position of maximum depth varying from 40% at the bottom to 25% at the top of the sails. This sail shape was chosen from available sail models.

Table 1. Principal Dimensions of the *Elliot 6m*.

Type	[-]	Keelboat
No. of Crew	[-]	3
Length over All	[m]	6
Beam Length	[m]	2.35
Max Draft	[m]	1.66
Dry Weight Boat	[kg]	635
Sailing Weight (w. Crew)	[kg]	840
Span	[m]	8.45
Mainsail Area	[m²]	15.9
Jib / Genoa Area	[m²]	7.7
Spinnaker Area	[m²]	28.0

Figure 3. *Elliot 6m*.

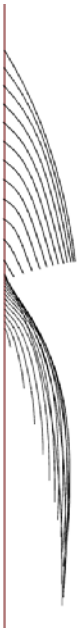

Figure 4. Mainsail and jib profiles.

For simplicity the sails of the *Elliot 6m* were modeled rigid and trimmed at constant settings.

SIMULATION SETUP

The simulations were performed using *STAR-CCM+8.02, a* viscous turbulent Finite Volume RANSE flow code. Therefore, a finite flow domain around the two boats had to be discretized by means of a volume grid. Flow physics were characterized by a steady, incompressible, single-phase, turbulent non-uniform flow. Turbulence was modeled by the Shear Stress

Transport model (SST). This blending of a *k-ε* and a *k-ω* turbulence model provided the best compromise for flow problems with dominant boundary layers and large free stream zones. Mass, momentum and turbulence equations were discretized using second order upwind differencing. Velocity-pressure coupling was accounted for with the SIMPLE algorithm (Semi-Implicit Method for Pressure-Linked Equations).

The incident flow has to resemble the condition of a boat moving on the water through the air. Therefore, the vertical change of wind speed as well as the wind twist had to be modeled. The logarithmic velocity profile was used to represent the variation of wind with elevation above water level. The true wind speed v_T is then:

$$v_T(z) = v_T(z = 10m)\frac{\ln(z / z_0)}{\ln(10m / z_0)} \tag{1}$$

where z denotes the height above water level. For the base roughness z_0 a value of z_0=0.0001 m was chosen. In the test case examined here, the true wind angle was assumed to be β_T = 40°. From true wind speed and angle, apparent wind speed and angle at each elevation were calculated with the following relationships, assuming a leeway angle of γ_S=0°:

$$v_A(z) = \sqrt{(v_T(z)\cos\beta_T + v_S)^2 + (v_T(z)\sin\beta_T)^2} \tag{2}$$

$$\tan\beta_A(z) = \frac{v_T \sin\beta_T}{v_T \cos\beta_T + v_S} \tag{3}$$

The apparent wind profile derived from (2) and (3) was used as the boundary condition of the inlet boundaries of the fluid domain. The true wind speed at a height of z=10 m was 7.77 m/s and the boat speed v_S =3.09 m/s. Based on these values the apparent wind angle at the 10 m elevation was β_A=25.20° and the apparent wind speed was v_A=10.33 m/s.

The computational domain was 80 m long, 60 m wide and 18 m high. The mesh in the area around the boats was refined to capture the interaction effect. Figure 5 shows the computational domain, with the refined area marked in magenta. The mesh in the vicinity of each boat was discretized even finer in order to resolve any local flow phenomenon.

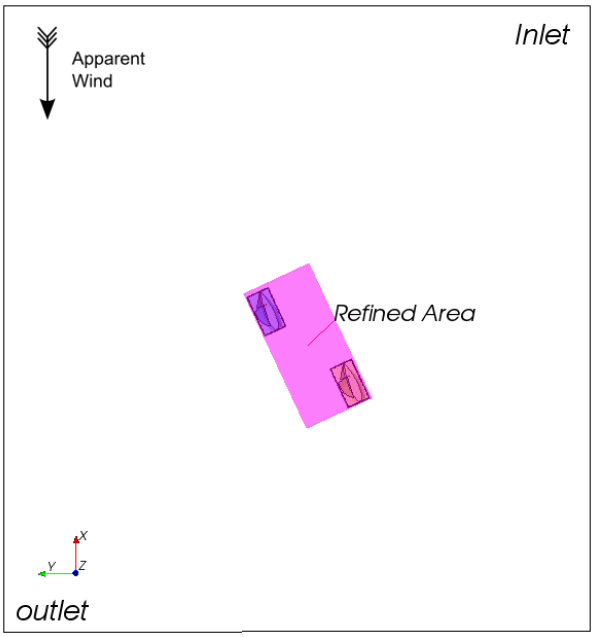

Figure 5. Computational domain, 80m in windward direction, 60m in transverse direction, height is 18m.

Depending on the distance between the boats and the resulting size of the refined area, grid sizes ranged from 7.5x10^6 to 40x10^6 computational cells, resulting in a system of nonlinear equations with 45 million to 240 million unknowns. The simulations were performed on a Linux computer cluster with about 100 cores. An individual simulation job was run on 24 to 32 cores, resulting in computational runtimes of approximately 2 to 10 hours.

RESULTS

Within this section the findings of the CFD investigations will be used to discuss the influence of the interference between the two boats on lift and drag. The resulting effect on aerodynamic thrust and boat speed will be highlighted.

Figure 6 shows contours of the local pressure reduced by the ambient pressure, p-p_A , on a plane at a height of 50% of the span of the boats. The wind is coming from the right, the leeward sailboat is about one times the span ahead of and about 0.5 times the span to leeward of the windward boat. The effect of aerodynamic interference is detected by comparing the pressure contours in the vicinity of the sails, in particular on the suction side.

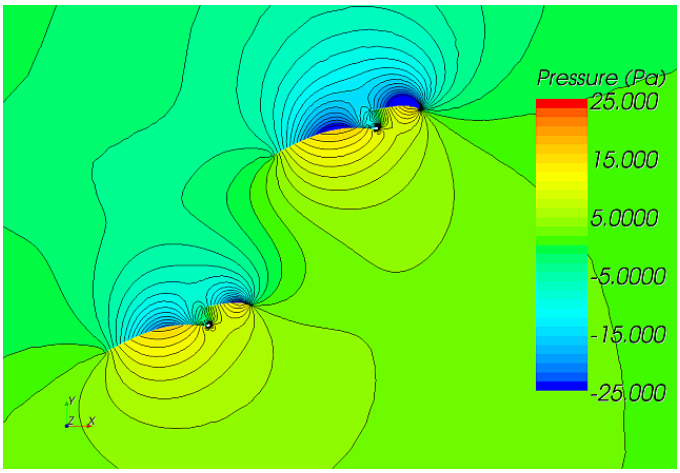

Figure 6. Pressure contour plot of leebow situation, shown on a horizontal plane at z = 0.5 span.

One can see that suction is considerably more pronounced on the leeward boat. This indicates an upwash from the trailing boat onto the sails of the leading boat.

For a quantitative assessment of the aerodynamic interference, the change in the driving force coefficient Δc_T of a target boat due to the existance of a second boat at various locations is calculated. Here the target boat is the blue boat according to Figure 2 and the second boat is the yellow one. The driving force coefficient is the aerodynamic force in the longitudinal direction of the boat, normalized by apparent wind speed at a height of 10m and the sail area.

$$C_T = \frac{F_L \sin\beta_A - F_D \cos\beta_A}{0.5\rho V_A^2 A_{Sails}} \tag{4}$$

In addition the change of boat speed of the target boat, ΔV_S, due to the change in driving force coefficient is predicted allowing a quantitative assessment of the impact of aerodynamic interference. To this end, the AVPP velocity prediction program was used (*Graf, 2005).*

VPP calculations were conducted in the following manner: for every aerodynamic lift and drag coefficient predicted from the RANSE calculation, a VPP run is conducted. Within a single VPP calculation, aerodynamic coefficients are kept constant.

Hydrodynamic forces are derived from a full set of coefficients, with the total hydrodynamic force in the direction of boat motion R_{Tot} calculated using:

$$R_{Tot} = R_U + R_H + R_I + \sum R_{PP} \tag{5}$$

Here R_{Tot} is total resistance, R_U is upright resistance at non-lifting condition, R_H is added resistance due to heel, R_I is induced resistance due to production of lift and R_{PP} is the parasitic profile drag of the keel fin and rudder profile. The heeling force $F_{H\beta}$ is calculated from:

$$F_{H\lambda_S} = (f_{H0} + \frac{\partial f_H}{\partial \gamma_S}\gamma_S)\ 0.5\rho u_B^2 \nabla_{CB}^{2/3} \tag{6}$$

where ∇_{CB} is canoe body's buoyancy and f_H is the heeling force coefficient. f_{H0} is the heeling force coefficient at zero leeway (γ_S = 0). The hydrodynamic coefficients are estimated using an empirical formulation based on *Delft Systematic Yacht Hull Series* (Keuning and Katgert (2008), and (Keuning and Kapsenberg (1995)). Boat velocity is calculated by balancing aerodynamic and hydrodynamic forces and moments as functions of boat states.

$$\Delta F(u_B, \gamma_S, \varphi) = F_{Aero} + F_{Hydro} = 0 \tag{7}$$

where u_B is boat speed, γ_S denotes leeway and φ heel angle. Although aerodynamic coefficients are constant for a single VPP calculation, changes in aerodynamic forces due to heel and leeway angle are accounted for. On average, heeling angle is 18°, and maximum differences are +1.9 and -3.3°. For a given state heeling differences between the interfering boats are even smaller. On average, $\Delta\varphi$ is 0.0018° with maximum difference of -1.5°. Therefore, differences in heel can be considered small enough to be negligible in the context of this study.

From the VPP results, derivatives $\partial V_S / \partial C_T$ are calculated. As stated above, the impact of any small change of the side force on the boat speed has been neglected, assuming that the hydrostatic stability is sufficient to avoid depowering.

Figure 7 shows a contour plot of thrust coefficient changes ΔC_T of the target (blue) boat, which is shown in the center of the diagram, due to the second (yellow) boat at positions given by abscissa and ordinate of the diagram. The contour plot indicates the effect of the second boat on the target boat. Abscissa and ordinate values have been normalized by the span of the sailboat.

The advantage for the target boat is largest when the second boat is trailing directly in the target's boat wake. Here ΔC_T, the change of driving force coefficient of target boat due to second boat, is up to 18%. When the second boat remains in the wake but is moving aft, the advantage for the target boat slowly degrades but persists for a significant distance. At a distance of 3.35 span ΔC_T is still 6%.

Figure 8 shows effect of aerodynamic interference on the boat speed as a difference between the speed of the target boat and the second boat, ΔV_S. Here blue regions depict areas where the target boat is more than 0.1 knots slower than the second boat and orange regions depict areas where the second boat is more than 0.1 knots slower than the target boat.

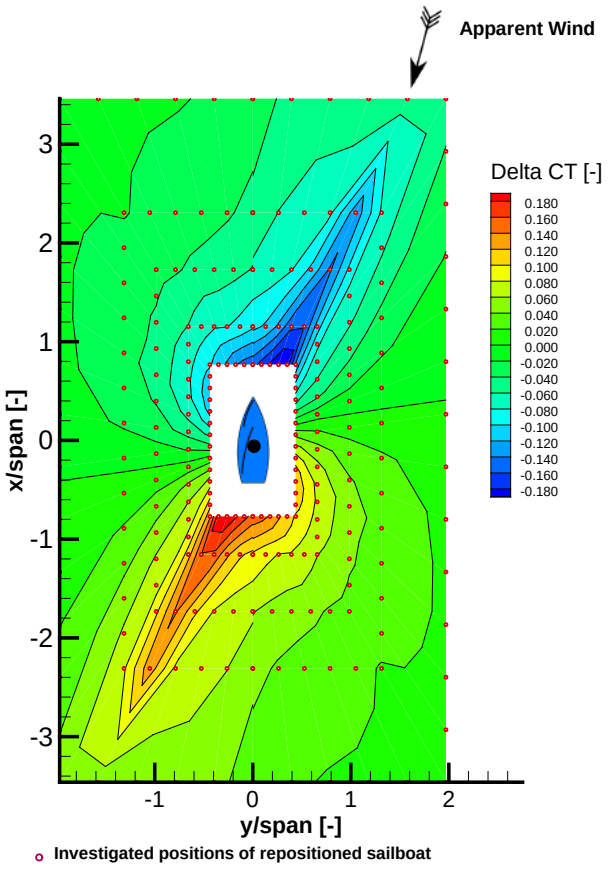

Figure 7. Contour plots of ΔC_T.

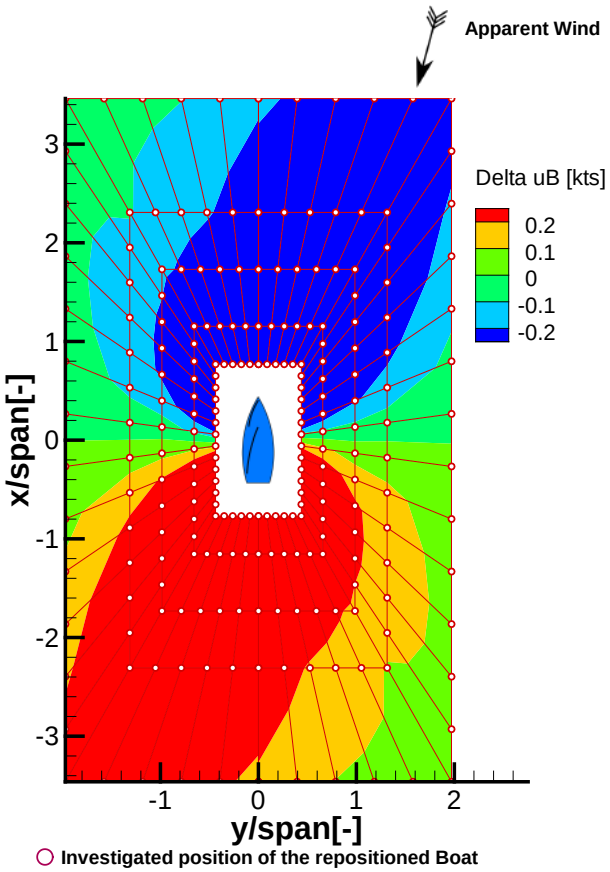

Figure 8. Impact of aerodynamic interference on boat speed

It can be observed that positions where the two boats are sailing directly abeam of each other, neither of them has a speed advantage. However, the leebow-position is advantageous as soon as the windward boat falls behind this point. If the windward boat is to weather of the leeward boat by 50% of its span and the leeward boat is behind by about 20% of the span, the leeward boat loses about 0.1 knots. If the windward boat is placed one span to windward of the target boat in a position even with respect to the true wind (on the same position with respect to a line perpendicular to the true wind – this is the classical start line position) a speed advantage of the leeward boat of about 0.2 knots is generated. Note that a speed difference of 0.1 knots lets the faster boat gain about one boat length for every two minutes of sailing. This is a huge advantage in a tactically critical situation, for example after the start of a race or when approaching the windward mark.

Figure 9 shows velocity streaks and a pressure plot for the situation where the second (yellow) boat is trailing directly behind the target (blue) boat. Velocity streak lines show the difference in apparent wind angle that the two boats encounter. Here the trailing boat suffers from a smaller angle of incidence on its sails due to a downwash from the sails of the blue boat. In the pressure plots, this results in a low pressure bubble on the pressure side of the fore sail which is indicated by the black arrow.

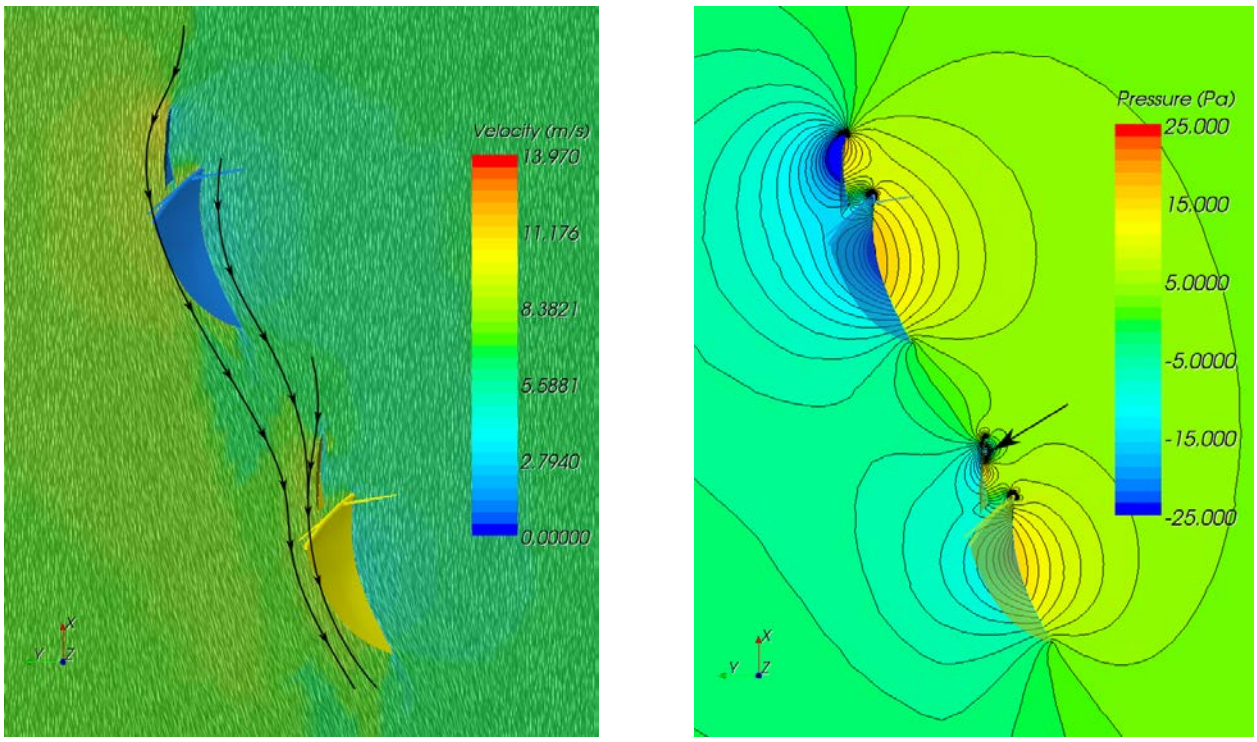

Figure 9. Velocity streaks and pressure contours on a plane at z=0.5 span. Situation: second boat directly trailing the target boat.

A comparison of the results with existing data is depicted in Figure 10. Richards (2013) presented data measured in the University of Auckland's twisted flow wind tunnel. The setup consisted of two similar models of modern racing sailboats. The models use semi rigid sails at an apparent wind angle of β_A=20° and a heel angle of 25°. The target model was fixed at the force balance of the wind tunnel. The second model was placed at various locations around the target model, the location described by the angle and radii of the second model's reference point with respect to the target model's reference point and its center line. Forces on the target model were measured and compared to a benchmark measurement which was investigated in the conventional isolated arrangement, i.e. without any aerodynamic interference. The data measured by the Yacht Research Unit of the University of Auckland is represented by the blue curve in Figure 9. The red curve represents data published by Caponnetto (1996), who investigated the interference between two IACC class yachts using a Vortex-Lattice code and rigid sails. The two sailboats were investigated sailing close-hauled at an apparent wind angle of β_A=25° and upright (heel angle = 0°). Finally, the green curve in Figure 10 shows the data from this study (β_A=25.2°, heel angle = 12.5°).

The diagram shows the ratio of the driving force of the target sailboat interfering with a second boat and the driving force of an isolated sailboat on the same track. This value is plotted over the directional angle of the two sailboats interfering (the angle between the centerline of the target boat and a line from a reference point on the target boat to the same point on the second boat). The distance between the reference points on the two boats is one times their span.

The results from the three sources are not strictly comparable, because the yachts / models are different as well as the investigation methods and the test setups. While the numerical methods use rigid sails, the wind tunnel investigation features semi-flexible sails and a rig which will deflect under load. In addition, the apparent wind angle and the heel angle differ. Some details of the flow conditions of the reference test results are not known - for example

the twist angle and the actual trim of the sails. In spite of these differences the similarities between the three methods are notable.

While the impact of interference on the target boat due to a second boat is negative over almost the entire range of directional angles, at angles between 100° and 180° the boat in a leebow position generates more driving force than an isolated boat. Consequently, it can be advantageous in a race to seek a leebow position, even if the windward boat is not the main competitor in the race.

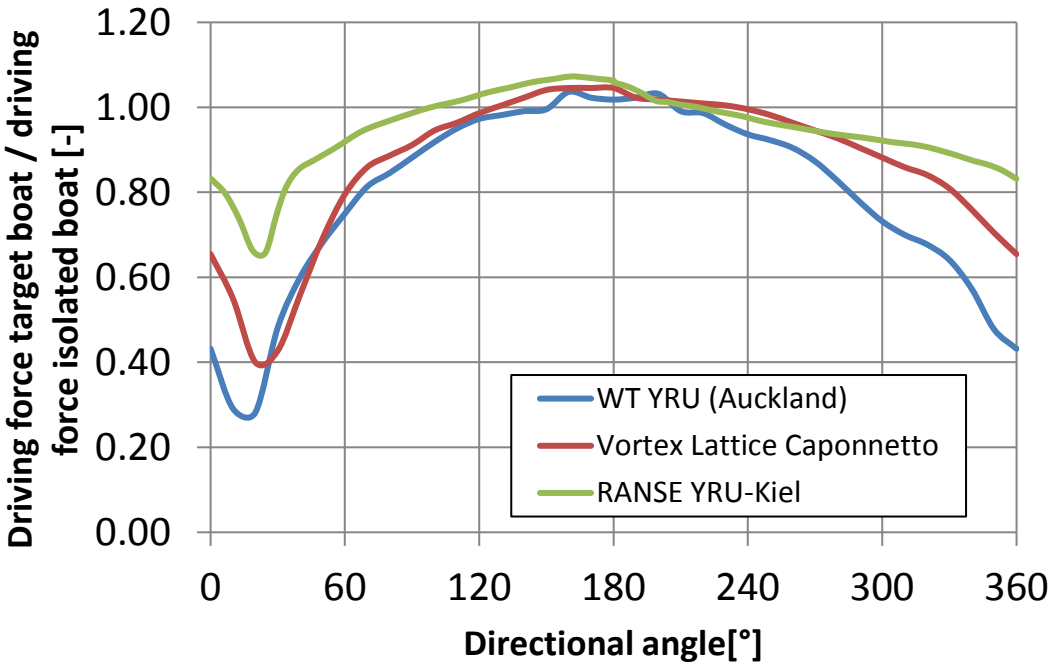

Figure 10. Comparison of driving force ratios.

A comparison of the results in Figure 10 shows that principle effects of interference on driving force are captured similarly for all three methods. However, the driving force ratio differs as much as 0.40. The difference is largest for small directional angles (i.e., one boat directly in front of or behind the other). Here, the wind tunnel data give a driving force ratio of 0.43, while RANSE CFD gives 0.83. The Vortex lattice method predicts a ratio 0.65 which is right between the two other methods. A reason for this may be that soft sails in the wind tunnel tests will luff on the target boat when the second boat is directly in front of it. All three curves show a local minimum at 20° to 30°. Thereafter, differences between the methods quickly become smaller. For 180°, differences between the methods have virtually vanished. After that point, the wind tunnel data shows a rapid decrease in driving force ratio while the CFD data show a gentler slope.

The results of the three methods compared here are generated with different types of sailboat models and different sailing parameters. Differences in rig geometries are listed in Table 2. The apparent wind angle is 20° for the wind tunnel test while it is about 25° for both CFD simulations. This might be the reason for the different directional angle at which the minimum driving force ratio occurs. The directional angle at minimum driving force ratio is 17° for the wind tunnel results, 23° for the vortex-lattice method and 22° for RANSE CFD. Heel angle differs from 25° for the wind tunnel study to 12.5° for the RANSE CFD to 0° for the vortex lattice method. Unfortunately, sail shape related parameters like maximum camber, camber position, trim angles and twist ratios are not available for the comparison cases.

Table 2. Comparison of rig geometries used in the three different cases.

			Capponetto IACC	Richards	YRUK *Elliot 6m*
Apparent Wind Angle	$ß_A$	[°]	25	20	25.2
Heel Angle	φ	[°]	0	25	12.5
Mast Height	h	[m]	32.50	?	8.45
Main Sail Area	A	[m²]	212.00	?	15.90
Aspect Ratio	AR= h²/A	[-]	4.98	?	4.49

Additional reasons for the differences of the RANSE CFD results and the comparison cases may be wake effects. RANSE CFD results take full scale Reynolds number (of an Elliot yacht) into account, while wind tunnel tests are performed at model scale and vortex lattice methods do not take viscosity into account at all.

Beside the inherent differences in the employed methods (experiment, inviscid flow simulation and viscous flow simulation), another possible explanation is differences in sail shape parameters between the compared cases. Naturally, the predefined sail shape has a great influence on overall sailboat performance. Here future RANSE simulations of trim configurations as a function of apparent wind angle, sail camber, camber position and twist could bring interesting insights.

CONCLUSIONS

Within this paper aerodynamic interference between two sailboats was investigated. The sailboats were sailing close-hauled and were located at different distances and angles to each other. Positive and negative interference effects on the driving force were evaluated, with special focus on the so-called leebow situation.

The simulations showed that differences in driving force are largest when one boat sails directly in the wake of another. For the classic leebow-position speed differences of 0.1 to 0.2 knots were predicted. The advantage of a leebow-position begins as soon as a windward boat falls behind with respect to a line perpendicular to the centerline of the leeward sailboat.

The findings from the simulations were compared with two similar studies conducted with different methods. In general, qualitative agreement between the methods was found to be very good. However, quantitavive differences of up to 0.4 in drive ratio were found. The most likely reasons for these differences are differing investigation methods as well as the difference in sail shapes and trims of the sails.

With respect to further studies, it would be interesting to control the conclusion stated above by repeating the investigation with identical sail shapes and trims for all methods. Furthermore, it would be interesting to conduct a similar study for downwind sails.

Acknowledgements

This study is part of the *PerforManD* project which is funded by the INTERREG4A program of the European Union.

INTERREG4A SYDDANMARK-SCHLESWIG-K.E.R.N.

European Regional Development Fund
European Union · Investing in your future

REFERENCES

Richards, P. J., Le Pelley, D. J., Jowett, D., Little, J. and Detlefsen, O. (2013). “A wind tunnel study of the interaction between two sailing yachts,” *Proceedings of the 21st Chesapeake Sailing Yacht Symposium*, Annapolis, MD.

Caponnetto, M. (1996). “The aerodynamic interference between two boats sailing close-hauled”, *International Shipbuilding Progress*, 44(439), 241-256.

Graf, K. and Böhm, C. (2005): "A New Velocity Prediction Method for Post-Processing of Towing Tank Test Results", *Proceedings of the 17th Chesapeake Sailing Yacht Symposium*, Annapolis, MD.

Keuning, J.A. and Katgert, M. (2008): “A Bare Hull Resistance Prediction Method Derived from the Results of the Delft Systematic Yacht Hull Series Extended to Higher Speeds”, *Proceedings of the International Conference on Innovation in High Performance Sailing Yachts*, Lorient, France.

Keuning, J.A. and Kapsenberg, G. (1995): “Wing-body Interaction on a Sailing Yacht”, *Proceedings of the 12th Chesapeake Sailing Yacht Symposium*, Annapolis, MD.